ELSEVIER

Clinical Neurophysiology 111 (2000) 2245–2254

www.elsevier.com/locate/clinph

Transient global ischemia specifically modulates visual P300 scalp distribution

Markus Ullsperger[a,b,*], Axel Mecklinger[a], Gabi Matthes-von Cramon[b], D. Yves von Cramon[a,b]

[a]*Max-Planck-Institute of Cognitive Neuroscience, Leipzig, Germany*
[b]*Day-Care Clinic for Cognitive Neurology, University Leipzig, Leipzig, Germany*

Accepted 15 September 2000

Abstract

Objective: Latency, amplitude, and scalp topography of the visual P300 component was examined in patients who had suffered from transient global ischemia (TGI) due to cardiac arrest and in age matched clinical and healthy controls in order to investigate the diagnostic value of this component.

Method: Event-related potentials (ERPs) were recorded from 19 scalp electrodes in a visual oddball paradigm.

Results: Mean latency of the P300 component was prolonged in both patient groups. Changes in scalp distribution of the P300, however, appear to be specific to anoxic-ischemic encephalopathy. In particular, a selective reduction of the P300 amplitudes at posterior recording sites was observed in TGI patients. Moreover, examination of the auditory P300 in TGI patients revealed that this selective change seems to be restricted to the visual modality.

Conclusion: The results are discussed with respect to selective vulnerability of brain tissue to hypoxic-ischemic injury. After TGI a modality-specific subset of P300 generators, probably located in the transitional parieto-occipital and extrastriate occipital cortex, appears to be affected. It is also noted, that the visual P300 component could serve as an additional marker of TGI especially in patients who do not show neuropathological changes in structural brain images.

Keywords: Event-related potentials; P300; Anoxic encephalopathy; Transient global ischemia

1. Introduction

Transient global ischemia (TGI) due to cardiac arrest may result in structural damage of brain tissue and profound neuropsychological disorders. The lack of blood and oxygen supply of the brain leads to localized and non-localized lesion patterns, resulting in anoxic encephalopathy. The extent of the structural damage caused by global ischemia depends on a number of factors, as (1) duration, (2) the completeness of ischemia, (3) brain temperature, and (4) blood glucose level (Auer and Beneviste, 1997). If the blood flow is restored before a critical time point varying with the other 3 factors, the cardiac arrest will not lead to death, but various ischemic tissue injuries develop. As revealed by neuropathological post-mortem studies, TGI gives rise to laminar or focal necrosis in specific, selectively vulnerable neuroanatomical regions: the cerebral cortex, hippocampus, and cerebellum (e.g. Auer and Beneviste, 1997; Zola-Morgan et al., 1986; Cervós-Navarro and Diemer, 1991; Kuroiwa and Okeda, 1994; Petito et al., 1987). The basal ganglia may also be affected. In the cortex, damage is most pronounced along the arterial boundary zones of the hemispheres. If the cessation of the cerebral blood flow is less prolonged, ischemic neuronal alteration is accentuated in the triple watershed zone, a region located more posteriorly than often realized - in the transitional parieto-occipital area; it is supplied by the most distal branches of the anterior, middle, and posterior cerebral arteries (Auer and Beneviste, 1997). Selective vulnerability of this cortical area is also supported by the finding that some survivors of cerebral hypoxia have visuospatial deficits (Volpe et al., 1986). In more severe cases, the cortical damage extends on a large territory in symmetrical distribution along the border zones of the large arteries (Auer and Beneviste, 1997; Cervós-Navarro and Diemer, 1991).

Neuropsychological tests can reveal a variety of impairments in memory and executive functions (Volpe et al., 1986; Kapur, 1988; Wilson, 1996; Mecklinger et al., 1998), but neuroimaging methods often fail to show pronounced lesions after TGI.

* Corresponding author. Max-Planck-Institute of Cognitive, Neuroscience, P.O. Box 500 355, D-04303 Leipzig, Germany. Tel.: +49-341-9940-262; fax: +49-341-9940-221.

E-mail address: ullsperg@cns.mpg.de (M. Ullsperger).

1388-2457/00/$ - see front matter CLINPH 2000610
PII: S1388-2457(00)00480-6

The aim of the present study was to examine whether event-related brain potentials (ERPs) might reveal diagnostically useful changes after TGI. ERPs are small-voltage oscillations measured non-invasively at the scalp that are time-locked to the processing of external events. Differences in timing and scalp topography of particular ERP components allow inferences about the timing and spatial characteristics of brain activity involved in cognitive processing (Rugg and Coles, 1995). The present study investigated the effect of TGI on the P300 component recorded in a visual classification (i.e. oddball) task. The P300 is a positive potential with a peak latency between 300 and 1000 ms elicited by attended, task-relevant, rare target stimuli. The P300 has been associated with memory access processes and is assumed to be proportional to the amount of revision or updating of a mental model in working memory (Mecklinger and Ullsperger, 1993; Donchin and Coles, 1988). A variety of data suggests that the scalp-recorded P300 results from the summation of a number of different neural generators (Johnson, 1993, 1995; Knight et al., 1989; Mecklinger and Ullsperger, 1995) some of which are assumed in the prefrontal cortex (Wood and McCarthy, 1985; McCarthy et al., 1996), the temporo-parietal junction area (Knight et al., 1989; Yamaguchi and Knight, 1992; Opitz et al., 1999), and the medial temporal lobe (Halgren et al., 1980, 1995). Although scalp topographies of the P300 component elicited by visual and auditory stimuli have more similarities than differences (Ji et al., 1999), brain lesion studies suggest that modality specific generators in primary and secondary association cortex contribute to the parietal maximal P300 such that for the visual P300 a contribution from extrastriate cortex can be assumed (Knight, 1997; Knight and Scabini, 1998). The P300 has been considered as the relevant dependent variable in the present study, because it is the most salient and robust endogenous ERP component and has already successfully been used as a diagnostic tool for a variety of neurological diseases (Ollo et al., 1991; Johnson et al., 1991, 1993).

The scalp topography of the target P300 component is age-dependent. While in young healthy persons the P300 has a focus over parietal brain regions, beginning in middle age the topographic distribution becomes more equipotential across the scalp midline (Friedman et al., 1997). This topographical change has been related to an age-related decline in efficiency of frontal lobe function (Fabiani et al., 1998).

In a recent study, Mecklinger et al. (1998) found a latency delay and a clearly different scalp topography of the P300 component in TGI patients compared to controls. Damage of the posterior parietal and occipito-parietal regions at the triple boundary zone of the 3 cerebral arteries could deteriorate the activation of putative cortical P300 generators located in or near that area. The present study aims at extending these findings by investigating a larger group of TGI patients, by adding an age-matched group of clinical control subjects, and by examining the P300 in an auditory oddball paradigm. This enables us to assess the specificity of scalp topography changes to TGI and also to disentangle these topographical changes from age-related changes of P300 scalp distribution.

2. Methods

2.1. Subjects

Three groups of subjects participated in the experiment: (1) a group of 13 patients, all of whom had suffered a period of TGI due to cardiac arrest (TGI group, two females); (2) a group of 8 neurological patients with brain lesions not resulting from TGI (clinical controls, 3 females) (Seven of these patients also participated in the study reported by Mecklinger et al. (1998)); and (3) 9 healthy controls (two females). The main clinical data and the brain lesions at the time of the study are reported in Table 1 for the TGI patients and in Table 2 for the clinical control patients. The groups were age-matched: the mean age amounted to 44.1 years (range: 19–59, SD = 12.6) in the TGI group, 42.0 years (range: 19–50, SD = 10.2) in the clinical control group, and 42.4 (range: 21–56, SD = 11.1) in the healthy control group. The patient groups were also matched for socioeconomic status (mean educational years: TGI group: 10.5 (SD = 2.9), clinical controls: 11.0 (SD = 2.7)) and intelligence assessed by the MWT (Mehrfachwahl–Wortschatz-Test; Lehrl et al., 1995; MWT-A score: TGI group: 98.5 (SD = 17.3), clinical controls: 103.0 (SD = 17.0)). Note that in none of the patients who had suffered from TGI structural neuroimaging revealed any significant change in signal intensity which could have been due to TGI. The neuropathology in the clinical control group ranged from vascular to inflammatory diseases of the central nervous system. The visuospatial functions as assessed by copying abilities in the Rey–Osterrieth Complex Figure Test (Spreen and Strauss, 1991) did not differ significantly between both clinical groups (mean score TGI group: 32.0 (SD = 6.2); clinical controls: 34.7 (SD: 1.3); $P = 0.24$). Each subject gave written informed consent prior to participation in the study, which was approved by the ethics committee of the Max Planck Institute of Cognitive Neuroscience.

2.2. Procedure and data recording

Subjects were comfortably seated in an acoustically and electrically shielded, dimly lit chamber, 0.9 m from the computer monitor. All stimuli were presented on a 17″ VGA monitor under the control of a Pentium computer. The stimuli consisted of simple 16 geometrical figures (cross, triangle, ring, etc.). Three hundred objects were presented in random order in the center of the screen, each for 200 ms and with an interstimulus interval of 1200 ms. Twenty-five percent of the objects were easily discernible through an opening (e.g. a ring) and the subject's

Table 1
Individual patient information for the 13 hypoxic patients under investigation[a]

	Patient												
	2	22	32	51	67	92	160	190	215	241	281	367	384
(A) Main clinical data													
Age (years)	43	48	46	19	39	46	37	55	59	21	51	51	57
Sex	F	M	M	F	M	M	M	M	M	M	M	M	M
Cardiac arrest	+	+	+	+	+	+	+	+	+	+	+	+	+
Functional causes	Toxic	toxic	DCM	El	CHDIMI	CHD/MI	CHD	DCM	CHD/MI	CC	Cl-ID/MI	CHD/MI	CHD/MI
Implementation of CPR	Unknown	Delayed	Delayed	Delayed	Instantly	Delayed	Delayed	Delayed	Delayed	Delayed	Delayed	Delayed	Instantly
Time since cardiac arrest (months)	31	9	12	5	6	36	5	6	17	6	7	6	24
(B) Neuropsychological data													
MWT	93	92	95	92	88	75	95	95	123	81	123	95	134
R–O	36	34	–	36	32	14	30	32	36	35	35	28	36

[a] CC, cardiac contusion, CHD, coronary heart disease; CPR, cardiopulmonary resuscitation; DCM, dilational cardiomyopathy; EI, electrical injury; MI, myocardial infarction; toxic, proarrhythmic drugs; MWT, Mehrfachwahl-Wortschatz-Test (Lehrl et al., 1995); R-O, copying ability score in Rey-Osterrieth complex figure test (Spreen and Strauss, 1991).

Table 2
Individual patient information for the 8 clinical control patients under investigation[a]

	Patient							
	109	115	130	131	141	147	148	164
(A) Main clinical data								
Age (years)	50	50	45	42	38	19	44	48
Sex	M	F	M	M	M	F	F	M
Diagnosis	Infarction of left PCA	Infarction of boundary zone ACA/MCA	ICH left posterior thalamus, mt. capsule	Left ATL	MS	ADEM	SAH (ruptured aneurysm of right MCA)	HSV-meningo-encephalitis
Time since brain lesion (months)	18	13	22	10	12	8	20	6
(B) Neuropsychological data								
MWT	125	98	80	91	126	88	112	104
R–O	35	36	36	35	34	32	35	35

[a] ADEM, acute demyelinating encephalomyelitis; ACA, anterior cerebral artery; HSV, Herpes simplex virus; ICH, intracerebral hemorrhage; MCA, middle cerebral artery; MS, multiple sclerosis; PCA, posterior cerebral artery; SAH, subarachnoideal hemorrhage; MWT, Mehrfachwahl-Wortschatz-Test (Lehrl et al., 1995); R-O, copying ability score in Rey-Osterrieth complex figure test (Spreen and Strauss, 1991).

task was to count these target objects and to report the result afterwards.

The EEG activity was recorded (band pass from DC to 30 Hz) with 19 electrodes referenced to the left mastoid. Vertical and horizontal eye movements were recorded with two pairs of electrodes placed on supra- and suborbital ridges and the outer canthus of each eye. Electrode impedance was kept below 5 KOhms. The EEG was A–D converted with 16 bit resolution at a sampling rate of 250 Hz and offline referenced to linked mastoids.

2.3. Data analysis

ERPs time locked to targets and standards were computed from 200 ms before stimulus onset until 1000 ms thereafter. The average voltages in the 200 ms preceding stimulus onset served as a baseline. Whenever the SD in a 200 ms time interval exceeded 40 μV the epoch was rejected. The number of rejected trials did not differ between patients and controls. The subject average ERPs were digitally low-pass filtered at 12 Hz (cut-off frequency). The P300 components were measured as mean voltages in the 300–600 ms time intervals. The peak latency was defined as the time point of the maximal positive deflection within this time interval. For statistical analysis, 11 electrodes, including the 3 midline sites Fz, Cz and Pz, as well as bilateral frontal (F3, F4), central (C3, C4), parietal (P3, P4), and occipital sites (O1, O2), were selected. The ERP data were subjected to repeated-measures ANOVA with Huynh–Feldt corrections (Huynh and Feldt, 1970) for inappropriate degrees of freedom due to violations of the sphericity assumption. Scalp potential topographic maps were generated using a two-dimensional spherical spline interpolation (Perrin et al., 1989).

3. Results

All patients except for one (Patient 32, who could nevertheless discriminate between standards and targets) and all control subjects reported the correct number of targets. The ERP waveforms elicited by the visual target and standard stimuli and the topographical maps of the target P300 in all 3 groups are displayed in Figs. 1–3.

The mean peak latencies of the target and standard P300 at the Pz electrode are shown in Table 3. The latencies were around 35 ms longer in both patient groups compared with the controls. This was confirmed by a two-way ANOVA with the between-subjects factor group (3 levels) and the within-subjects factor stimulus type (two levels) revealed a main effect of group for P300 latency ($F(2, 27) = 5.71$; $P < 0.01$). Post-hoc tests showed, that P300 latencies in the healthy control group were significantly shorter than in the other two groups (TGI group vs. healthy controls: $F(1, 20) = 6.25$, $P < 0.05$; clinical controls vs. healthy controls: $F(1, 15) = 9.89$, $P < 0.01$). The latencies of the P300 obtained in the TGI and the clinical control groups did not differ significantly ($P = 0.14$).

As is apparent from Fig. 1, in the TGI group the P300 amplitude to both types of stimuli is selectively reduced at posterior recording sites, whereas the relative amplitudes at central and frontal electrodes are comparable in all 3 groups.

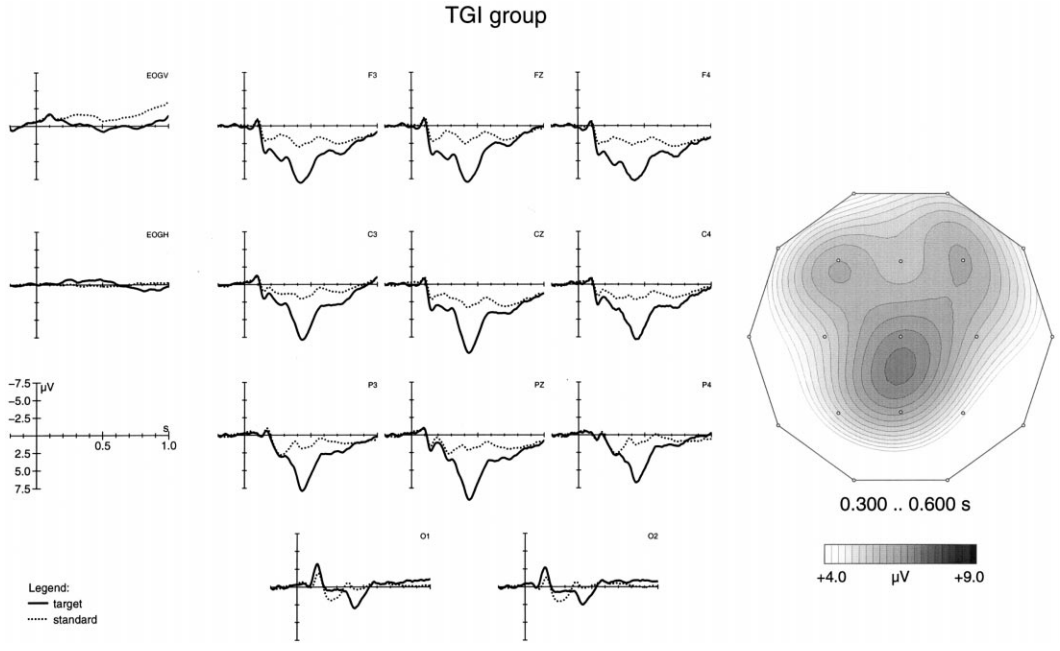

Fig. 1. ERP waveforms averaged across TGI patients elicited by visual target and standard stimuli (left side); topographic maps of the visual target P300 scalp distribution in the latency range 300–600 ms (right side).

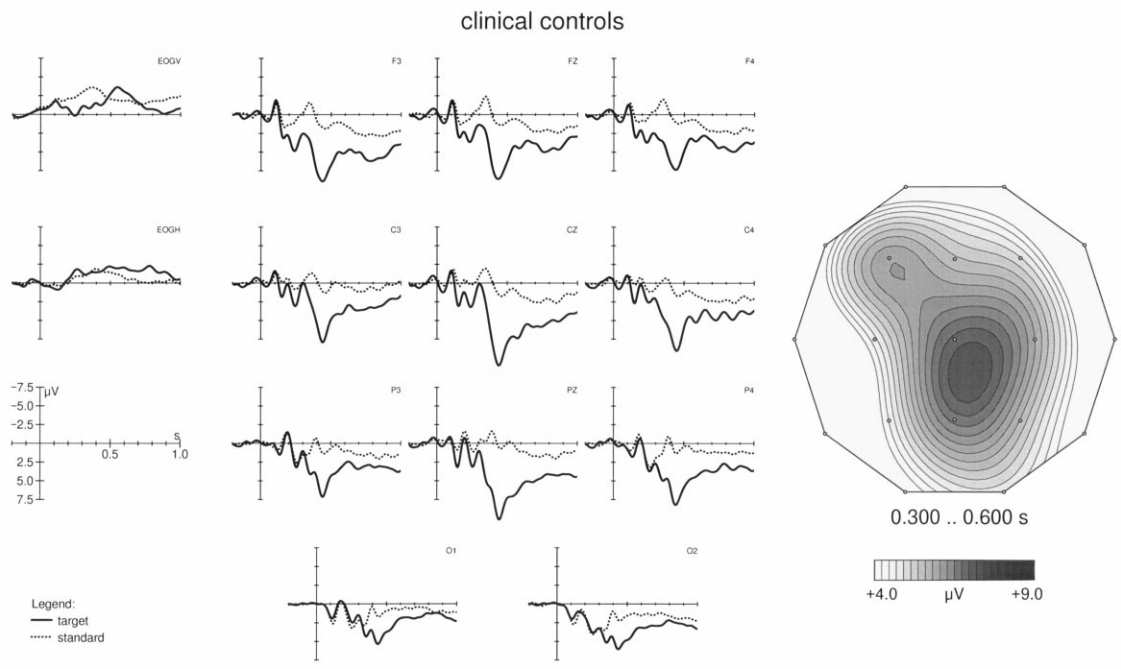

Fig. 2. ERP waveforms averaged across control patients elicited by visual target and standard stimuli (left side); topographic maps of the visual target P300 scalp distribution in the latency range 300–600 ms (right side).

This topographical difference is illustrated in Fig. 4, which displays the mean amplitudes for the target P300 at the 3 midline electrodes and O1 and O2. The difference in scalp topography was confirmed by an ANOVA with the between-subjects factor group (3 levels) and the within-subjects factors electrode (11 levels) and stimulus type (two levels), which revealed a significant interaction electrode × group ($F(20, 270) = 2.77$; $P < 0.01$). Based on the latter interaction, separate ANOVAs (stimulus type × electrode × group) were performed to contrast the groups. The interaction electrode × group was significant when contrasting the TGI with the healthy control group

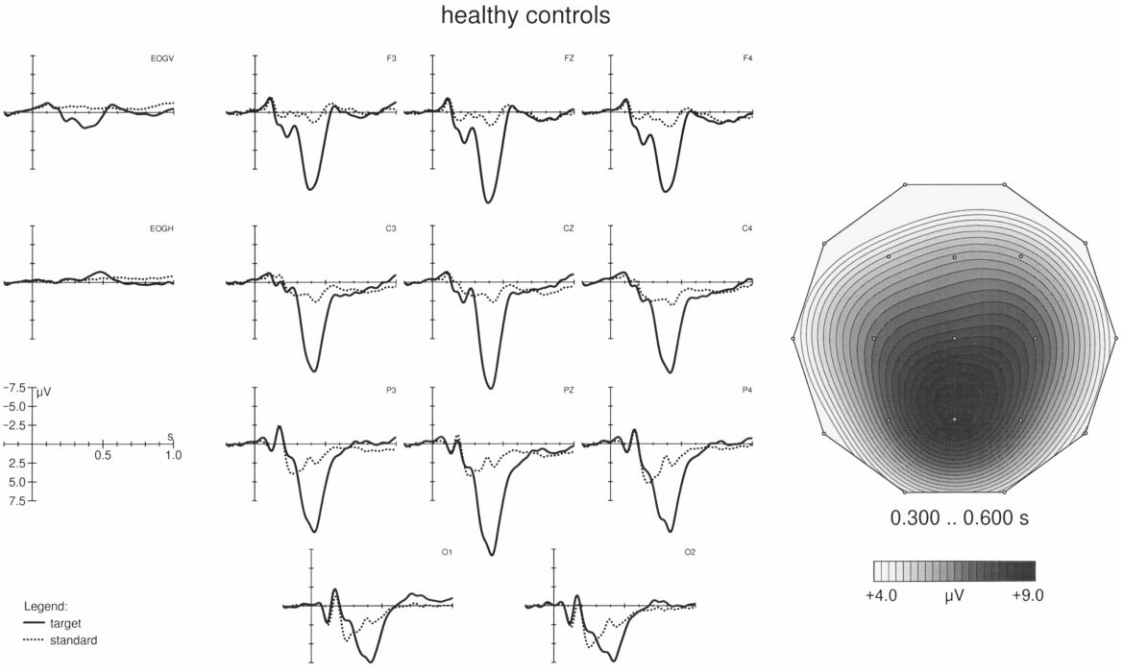

Fig. 3. ERP waveforms averaged across healthy controls elicited by visual target and standard stimuli (left side); topographic maps of the visual target P300 scalp distribution in the latency range 300–600 ms (right side).

Table 3
Mean peak latencies of the target and standard P300 at the Pz electrode in the 3 groups[a]

	TGI group	Clinical control group	Normal control group
Target P300 latency (ms)	441 (6.2)	456 (19.0)	418 (4.4)
Standard P300 latency (ms)	444 (12.8)	449 (7.2)	414 (14.4)

[a] The standard error of the mean is presented in parentheses.

($F(10,200) = 3.89$, $P < 0.05$) and the TGI with the clinical control group ($F(10,190) = 2.40$, $P < 0.05$), while the same ANOVA contrasting the two control groups did not reveal a significant interaction electrode × group ($F(10,150) = 1.62$, $P = 0.141$). After removal of between-group differences in P300 amplitude (cf. McCarthy and Wood, 1985), the same significant interactions were obtained (TGI vs. healthy controls: $F(10,200) = 4.70$, $P < 0.005$; TGI vs. clinical controls: $F(10,190) = 2.37$, $P < 0.05$), indicating that different neuronal generators contribute to the visual P300 in posthypoxic patients and the other two groups. In addition, planned comparisons contrasting the P300 amplitude at occipital electrodes at which the between-group differences were largest for the TGI and the two control groups revealed significant main effects of group (TGI vs. healthy controls: $F(1,20) = 9.69$, $P < 0.01$; TGI vs. clinical controls: $F(1,19) = 5.18$, $P < 0.05$), whereas no significant difference was found when the two control groups were contrasted ($F(1,15) = 0.04$, $P = 0.84$). These findings further support the view, that the differences in scalp topography of the P300 component result from a selective reduction of the amplitude at posterior recording sites in the TGI group compared to the control groups.

One explanation of the findings could be that the topographical changes of the visual P300 after transient global ischemia are due to a hippocampal damage. Several postmortem studies described a selective vulnerability of the hippocampus (particularly the CA1 region) to hypoxia (e.g. Auer and Beneviste, 1997; Zola-Morgan et al., 1986; Cervós-Navarro and Diemer, 1991; Kuroiwa and Okeda, 1994; Petito et al., 1987). Moreover, intracranial recordings in the hippocampus in epileptic patients revealed in oddball tasks, in both visual and auditory modality, a large negative component that is considered the hippocampal equivalent to the scalp recorded P300 (McCarthy et al., 1989; Grunwald et al., 1999). While it can be assumed that the hippocampus proper forms a closed field and has no direct influence on the scalp recorded P300, it is still conceivable that damage of the hippocampal formation and its cortico-cortical fiber projections might lead to topographical changes as found in our TGI patients. This argument, however, should hold for the P300 component elicited by auditory stimuli as well. That means, TGI patients should show a similar topographical modulation of the auditory P300. Therefore we compared the scalp distribution of the P300 component recorded in an auditory oddball paradigm using 600 Hz tones as standards (80%) and 800 Hz tones as the to-be-counted targets (20%) in 8 TGI patients (patients 22, 160, 190, 215, 241, 281, 367, 384) and 8 healthy controls (Note that for the healthy controls the target and standard ERPs were recorded in a novelty paradigm, in which in addition to standard and target tones novel sounds were presented with low frequency. To our knowledge the presence or absence of novel sounds does not alter the P300 to target tones, neither in latency nor in topography. The response requirements were the same for the patients' (two tone) and the controls' (two tone plus novels) experiments. Mainly for these reasons we considered the controls' target P300 as an adequate control for the patient group data.) matched for age, gender, and socioeconomic status. The waveforms and the scalp topographies are displayed in the Figs. 5 and 6. Statistical analysis was performed similarly as for the visual P300 component. No significant interaction electrode × group was found ($P = 0.59$), also normalized data did not give rise to an interaction of these factors ($P = 0.30$).

Finally, an ANOVA contrasting the scalp topographies of the visual and the auditory P300 in the 8 TGI patients revealed a significant interaction electrode × modality ($F(10,70) = 6.40$; $P < 0.005$; for normalized data: $F(10,70) = 5.29$; $P < 0.001$). Planned comparisons at occipital electrodes gave rise to a significant main effect of modality ($F(1,7) = 9.53$, $P < 0.05$). This is an important finding because it indicates that in TGI patients only the visual P300 is reduced at posterior recordings. This modal-

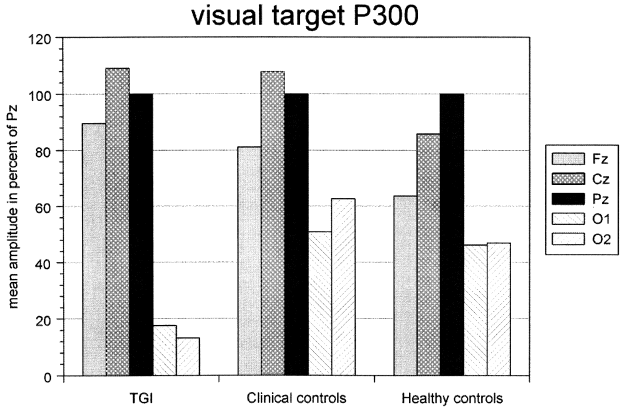

Fig. 4. Mean amplitudes for visual target P300 at Fz, Cz, Pz, O1, and O2 recorded in the 3 groups. The amplitudes were normalized by converting them to the percentage of the P300 amplitude at Pz (cf. Johnson, 1993) to allow a better evaluation of topographical differences.

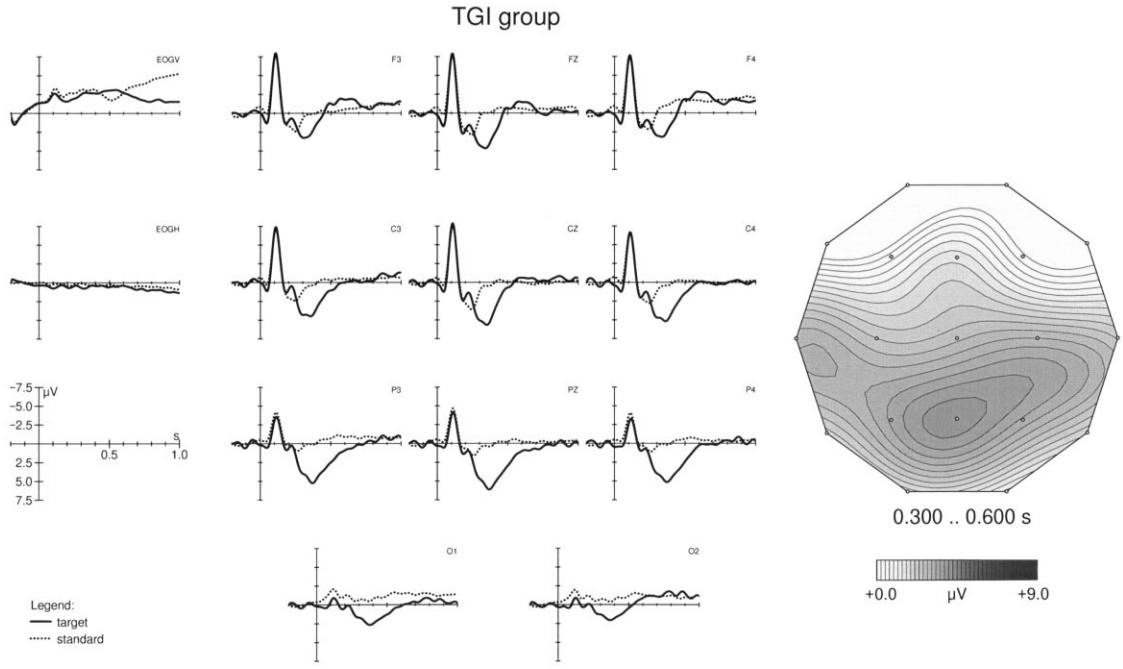

Fig. 5. ERP waveforms averaged across 8 TGI patients elicited by auditory target and standard stimuli (left side); topographic maps of the visual target P300 scalp distribution in the latency range 300–600 ms (right side).

ity-dependent difference in P300 topography stands in contrast to typical findings in healthy persons, who do not show significant topographical differences of the P300 components in auditory and visual oddball paradigms (e.g. Ji et al., 1999; Sangal and Sangal, 1996; Naumann et al., 1992).

4. Discussion

The present study was performed to examine whether various parameters of the P300 component are sensitive to brain lesions resulting from transient global ischemia. Based on neuropathological post-mortem findings in patients who

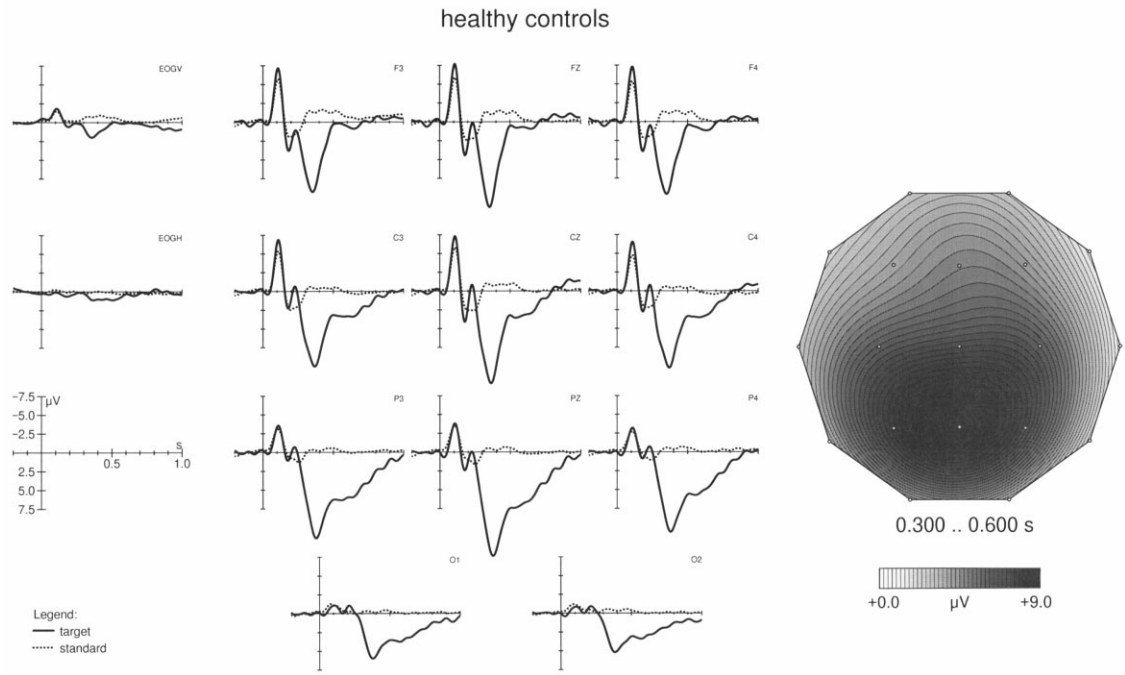

Fig. 6. ERP waveforms averaged across 8 healthy controls elicited by auditory target and standard stimuli (left side); topographic maps of the visual target P300 scalp distribution in the latency range 300–600 ms (right side).

had initially survived cardiac arrest indicating that the parieto-occipital area is vulnerable to TGI (Auer and Beneviste, 1997; Zola-Morgan et al., 1986), we hypothesized that visual P300 activity in TGI patients could be selectively modulated at posterior recording sites. While both clinical groups showed prolonged P300 latencies, it was only the TGI group that showed a different P300 scalp topography relative to the two other groups. The increased latency of the P300 component in both clinical groups reflects no alternative processes but a prolongation of stimulus evaluation. The topographical change in TGI patients was due to a selective reduction at posterior recording sites. Since all groups were matched for age, socioeconomic status and intelligence, these topography modulations cannot be attributed to differential age effects nor to unspecific factors. In 11 out of 13 TGI patients the amplitude of the visual P300 was larger at frontal and central electrodes compared to parieto-occipital recording sites, whereas only in two out of 9 healthy controls a similar topographical pattern was found, suggesting that even in single subjects topographic aspects of the P300 might be useful for assessment of presence or absence of anoxic-ischemic encephalopathy.

Considering the result that after TGI only the visual but not the auditory scalp recorded P300 is altered, the argument that hippocampal damage after TGI could have caused the change in scalp distribution seems very unlikely. Although it is not unequivocally possible to determine the generators responsible for the selective change of the P300 topography the data suggest that a modality-specific subset of P300 generators is affected by TGI. The selective amplitude reduction at posterior recordings might reflect a damage of the most vulnerable parts of the cerebral cortex, i.e. the triple boundary zone between the anterior, middle and posterior cerebral arteries. This triple watershed area lies in parieto-occipital and extrastriate occipital cortex, i.e. brain regions that have been identified as part of the neuronal network involved in the generation of the visual P300 (Knight, 1997). According to Knight et al. (1989); Verleger et al. (1994), auditory P300 activity is disproportionally reduced at posterior recordings in patients with discrete brain lesions at the temporo-parietal junction area. This region is not located in the triple watershed zone and should therefore be less vulnerable to cerebral ischemia. We suggest that the presumable pronunciation of hypoxic-ischemic tissue damage in the parieto-occipital cortex compared to other cortical regions (including the temporo-parietal junction) can explain, why only visual but not auditory P300 scalp topography is changed after TGI.

It is noteworthy, that neuroimaging studies did not show macroscopically visible structural brain damage in any of the 13 TGI patients under investigation, nor did our TGI patients show substantial visuospatial deficits as compared to clinical controls as revealed by the Rey-Osterrieth Complex Figure Test. Recent PET and SPECT studies (Kuwert et al., 1993; Rupright et al., 1996) found metabolic changes in the medial temporal cortex, but no significant changes in metabolism were obtained in frontal and parietal neocortical regions. Although there are some case reports about brain lesions following TGI visible in MRI (Sawada et al., 1990; Takahashi et al., 1998), in most cases structural MRI does not show severe pathological changes in survivors of cardiac arrests. Hence, the diagnostic value of structural brain imaging in TGI is limited. ERPs, particularly the visual P300 component, seems to be an easily performed and inexpensive, sensitive diagnostic measure for anoxic-ischemic encephalopathy.

Acknowledgements

We wish to thank Cornelia Schmidt for her valuable assistance in data collection.

References

Auer HN, Beneviste H. In: Graham DI, Lantos PL, editors. 6th. Greenfield's neuropathology1997. pp. 263–314.

Cervós-Navarro J, Diemer NH. Selective vulnerability in brain hypoxia. Crit Rev Neurobiol 1991;6:149–182.

Donchin E, Coles MGH. Is the P300 component a manifestation of context updating? Brain Behav Sci 1988;11:357–374.

Fabiani M, Friedman D, Cheng JC. Individual differences in P3 scalp distribution in older adults, and their relationship to frontal lobe function. Psychophysiology 1998;35:698–708.

Friedman D, Kazmerski V, Fabiani M. An overview of age-related changes in the scalp distribution of P3b. Electroencephalogr Clin Neurophysiol 1997;104:498–513.

Grunwald T, Beck H, Lehnertz K, Blumcke I, Pezer N, Kutas M, Kurthen M, Karakas HM, Van Roost D, Wiestler OD, Elger CE. Limbic P300s in temporal lobe epilepsy with and without Ammon's horn sclerosis. Eur J Neurosci 1999;11(6):1899–1906.

Halgren E, Squires NK, Rohrbough JW, Babb TL, Crandall PH. Endogenous potentials generated in the human hippocampal formation and amygdala by infrequent events. Science 1980;210:803–805.

Halgren E, Baudena P, Clarke JM, et al. Intracerebral potentials to rare target and distractor auditory and visual stimuli. II Medial, lateral and posterior temporal pole. Electroencephalogr Clin Neurophysiol 1995;94:229–250.

Huynh H, Feldt LS. Conditions under which mean square ratios repeated measurements designs have exact F distributions. J Am Stat Assoc 1970;65:1582–1589.

Ji J, Porjesz B, Begleiter H, Chorlian D. P300: the similarities and differences in the scalp distribution of visual and auditory modality. Brain Topogr 1999;11:315–327.

Johnson Jr R. On the neuronal generators of the P300 component of the event-related potential. Psychophysiology 1993;30:90–97.

Johnson Jr R. On the neuronal generators of the P300: evidence from temporal lobectomy patients. Electroencephalogr Clin Neurophysiol 1995;44S:110–129.

Johnson Jr R, Litvan I, Grafman J. Progressive supranuclear palsy: altered sensory processing leads to degraded cognition. Neurology 1991;41:1257–1262.

Johnson Jr R, Rohrbaugh JW, Ross JL. Altered brain development in Turner's syndrome: an event-related potential study. Neurology 1993;43:801–808.

Kapur N. Memory disorders in clinical practice, London: Butterworths, 1988.

Knight RT. Distributed cortical network for visual attention. J Cogn Neurosci 1997;9(1):75–91.

Knight RT, Scabini D. Anatomic bases of event-related potentials and their relationship to novelty detection in humans. J Clin Neurophysiol 1998;15:3–13.

Knight RT, Scabini D, Woods DL, Clayworth CC. Contributions of temporal-parietal junction to the human auditory P3. Brain Res 1989;502:109–116.

Kuroiwa T, Okeda R. Neuropathology of cerebral ischemia and hypoxia: recent advances in experimental studies on its pathogenesis. Pathol Int 1994;44:171–181.

Kuwert T, Hömberg V, Steinmetz H, et al. Posthypoxic amnesia: regional cerebral glucose consumption measured by positron emission tomography. J Neurol Sci 1993;118:10–16.

Lehrl S, Triebig G, Fischer B. Multiple choice vocabulary test MWT as a valid and short test to estimate premorbid intelligence. Acta Neurol Scand 1995;91(5):335–345.

McCarthy G, Wood CC. Scalp distributions of event-related potentials: an ambiguity associated with analysis of variance models. Electroencephalogr Clin Neurophysiol 1985;62:203–208.

McCarthy G, Wood CC, Williamson PD, Spencer DD. Task-dependent field potentials in human hippocampal formation. J Neurosci 1989;9(12):4253–4268.

McCarthy G, Luby M, Gore JC, Goldman-Rakic P. Functional magnetic resonance imaging in a visual oddball task. Neuroimage 1996;3:S548.

Mecklinger A, Ullsperger P. P3 varies with stimulus categorization rather than probability. Electroencephalogr Clin Neurophysiol 1993;86:395–407.

Mecklinger A, Ullsperger P. The P300 to novel and target events: a spatiotemporal dipole model analysis. NeuroReport 1995;7:241–245.

Mecklinger A, von Cramon DY, Matthes-von Cramon G. Event-related potential evidence for a specific recognition memory deficit in adult survivors of cerebral hypoxia. Brain 1998;121:1919–1935.

Naumann E, Huber C, Maier S, Plihal W, Wustmans A, Diedrich O, Bartussek D. The scalp topography of P300 in the visual and auditory modalities: a comparison of three normalization methods and the control of statistical type II error. Electroencephalogr Clin Neurophysiol 1992;83:254–264.

Ollo C, Johnson Jr R Gr, afman J. Signs of cognitive changes in HIV disease: an event-related brain potential study. Neurology 1991;41:209–215.

Opitz B, Mecklinger A, von Cramon DY, Kruggel F. Combining electrophysiological and hemodynamic measures of the auditory oddball. Psychophysiology 1999;36:142–147.

Perrin F, Pernier J, Bertrand O, Echallier JF. Spherical splines for scalp potential and current density mapping. Electroencephalogr Clin Neurophysiol 1989;72:184–187.

Petito CK, Feldmann E, Pulsinelli WA, Plum F. Delayed hippocampal damage in human following cardiorespiratory arrest. Neurology 1987;37:1281–1286.

Rugg MD, Coles MGH. The ERP and cognitive psychology: conceptual issues. In: Rugg MD, Coles MGH, editors. Electrophysiology of mind, event-related brain potentials and cognition, Oxford: Oxford University Press, 1995. pp. 27–39.

Rupright J, Woods EA, Singh A. Hypoxic brain injury: evaluation by single photon emission computed tomography. Arch Phys Med Rehabil 1996;77:1205–1208.

Sangal B, Sangal JM. Topography of auditory and visual P300 in normal adults. Clin Electroencephalogr 1996;27:145–150.

Sawada H, Udaka F, Seriu N, Shindou K, Kameyama M, Tsujimura M. MRI demonstration of cortical laminar necrosis and delayed white matter injury in anoxic encephalopathy. Neuroradiology 1990;32:312–319.

Spreen O, Strauss E. A compendium of neuropsychological tests. Administration, norms, and commentary, New York: Oxford University Press, 1991.

Takahashi W, Ohnuki Y, Takizawa S, et al. Neuroimaging on delayed postanoxic encephalopathy with lesions localized in basal ganglia. Clin Imaging 1998;22(3):188–191.

Verleger R, Heide W, Butt C, Kompf D. Reduction of P3b potentials in patients with temporo-parietal lesions. Cogn Brain Res 1994;2:103–116.

Volpe BT, Holtzman JD, Hirst W. Further characterization of patients with amnesia after cardiac arrest: preserved recognition memory. Neurology 1986;36:408–411.

Wilson BA. Cognitive functioning of adult survivors of cerebral hypoxia. Brain Inj 1996;10:863–874.

Wood CC, McCarthy G. A possible frontal lobe contribution to the scalp P300. Soc Neurosci Abstr 1985;11:879.

Yamaguchi S, Knight RT. Effects of temporal-parietal lesions on the somatosensory P3 to lower limb stimulation. Electroencephalogr Clin Neurophysiol 1992;84:139–148.

Zola-Morgan S, Squire LR, Amaral DG. Human amnesia and the medial temporal region: enduring memory impairment following a bilateral lesion limited to field CA1 of the Hippocampus. J Neurosci 1986;6:2950–2967.